Higgs Boson Production at the LHC with Soft Gluon Effects

C. Balázs[1,2] and C.–P. Yuan[3,4]
[1] *Department of Physics and Astronomy, University of Hawaii, Honolulu, HI 96822, U.S.A.*
[2] *Fermi National Accelerator Laboratory, Batavia, Illinois 60510, U.S.A.*
[3] *National Center for Theoretical Sciences, National Tsing-Hua University, Taiwan, Republic of China*
[4] *Department of Physics and Astronomy, Michigan State University, East Lansing, MI 48824, U.S.A.*
(January 12, 2000)

We present results of QCD corrections to Higgs boson production at the CERN Large Hadron Collider. Potentially large logarithmic contributions from multiple soft–gluon emission are resummed up to all order in the strong coupling. Various kinematical distributions, including the Higgs transverse momentum, are predicted at the $\mathcal{O}(\alpha_s^3)$ level. Comparison is made to outputs of the popular Monte Carlo event generator PYTHIA.

PACS numbers: 12.38.Cy, 14.80.Bn, 13.87.Ce, 13.85.Qk.
hep-ph/0001103, UH-511-951-00, FERMILAB-Pub-00/005-T, CTEQ-001, MSU-HEP/00103

I. INTRODUCTION

One of the fundamental questions of the Standard Model (SM) of elementary particle physics is the dynamics of the electroweak symmetry breaking. Within the SM, the Higgs mechanism postulates the existence of a scalar field, the elementary excitation of which is called the Higgs boson. Four experimental collaborations at the LEP II collider search for the Higgs boson in the $e^+e^- \to Z^0H$ process up to 202 GeV center of mass energy. DELPHI and L3 set a preliminary exclusion limit of $m_H > 96$ GeV on the Higgs mass, followed closely by the limit of $m_H > 91$ GeV set by ALEPH and OPAL [1]. According to recent preliminary information, the combined lower limit is close to $m_H \gtrsim 106$ GeV [2]. Global fits to electroweak observables appear to prefer a low mass Higgs particle, with a mean value close to 100 GeV, and less than 250 GeV within 95 percent of confidence [3,4].

Among other aims the main goal of the next proton-proton accelerator, the 14 TeV center of mass energy Large Hadron Collider (LHC) at CERN, is to establish the existence of the Higgs boson and to measure its basic properties. At the LHC a light SM Higgs boson will be mainly produced through the partonic subprocess gg (via top quark loop) $\to HX$ [5]. It can be detected, after about 1.5 years of running with a statistical significance of at least 4, in its $H \to \gamma\gamma$ decay mode, if its mass is in the 100-150 GeV range [6]. If the Higgs mass is higher than about 150 GeV, then its $H \to Z^{0(*)}Z^0$ decay mode is the cleanest and most significant [6]. In this letter our focus is on the Higgs boson production, and in our numerical illustration we choose $m_H = 150$ GeV.

According to earlier studies, a statistical significance on the order of 5-10 can be reached for the inclusive $H \to \gamma\gamma$ and for the $H+\text{jet} \to \gamma\gamma+\text{jet}$ signals, although actual values depend on luminosity and background estimates. In Ref. [7] it was found that in order to optimize the significance it is necessary to impose a 30 GeV cut on the transverse momentum of the jet, or equivalently (at next-to-leading order precision), on the transverse momentum (Q_T) of the photon pair. With this cut in place, extraction of the signal in the Higgs + jet mode requires the precise knowledge of both the signal and background distributions in the medium to high Q_T region.

To reliably predict the Q_T distribution of Higgs bosons at the LHC, especially for the low to medium Q_T region where the bulk of the rate is, the effects of the multiple soft–gluon emission have to be included. One approach to achieve this is parton showering [8]. Although the universality of this method makes it a very powerful tool, present drawbacks of this ansatz are the lack of the proper normalization (which takes into account the full fixed order QCD corrections), the lack of exact matrix elements even in the high Q_T region, and the lack of uniqueness of the prediction ("tunability"). There is ongoing work to correct these problems [9].

A more reliable prediction of the Higgs Q_T can be obtained utilizing the Collins-Soper-Sterman (CSS) resummation formalism [10,11], which takes into account the effects of the multiple soft–gluon emission while reproducing the rate, systematically including the higher order corrections. It is possible to smoothly match the CSS result to the fixed order one in the medium to high Q_T region, thus obtaining the best prediction in the full Q_T region [12]. Compared to fixed orders, the resummed result depends on a few extra parameters. These parameters are new renormalization scales (C_i, only two of which are independent) [11], and a few universal, non-perturbative parameters (g_i), which are extracted from present experiments and then used to predict the results of future ones [13]. In this letter, we use this formalism to calculate the total cross sections and Q_T distributions of Higgs bosons at the LHC.

Our results here, together with the resummed calculations for the diphoton and Z^0 boson pair production

[14–17], provide a consistent set of QCD calculations of the transverse momentum (and other) distribution(s) of the Higgs bosons and their backgrounds at the LHC. These results systematically include both the multiple soft–gluon effects and the finite order QCD corrections, and can be used to tune the shower MC's which experimentalists extensively use when extracting the Higgs signal, or can be utilized independently by means of the ResBos Monte Carlo event generator [12].

II. ANALYTICAL RESULTS

Within the SM [5,18], as well as in the minimal supersymmetric standard model (MSSM) with small $\tan\beta$ [5], the dominant production mode of neutral Higgs bosons at the LHC is gluon fusion via a heavy quark loop. The lowest order cross section of this process is formally $\mathcal{O}(\alpha_s^2)$ in the strong coupling. Fixed order QCD corrections to this production mechanism are known to substantially increase the rate. For a light Higgs boson the $\mathcal{O}(\alpha_s^3)$ to $\mathcal{O}(\alpha_s^2)$ K-factor is in the order of 2 (cf. Fig. 1). The full $\mathcal{O}(\alpha_s^4)$ calculation is not completed yet, but the real emission [19] and the virtual contributions [20] are separately available. Resummed calculations, taking into account the soft–gluon effect, were also performed to estimate the size of the uncalculated higher order corrections [21], as well as to predict the shape of the Higgs transverse momentum distribution [22,23].

In this work we use the Collins-Soper-Sterman (CSS) soft–gluon resummation formalism to calculate the QCD corrections from the multiple–soft gluon emission. Calculations similar to this were earlier performed in Refs. [22,23]. Our present calculation improves these by including $\mathcal{O}(\alpha_s^4)$ terms in the Sudakov exponent, by applying the state of the art matching to the latest fixed order distributions, by using a QCD improved gluon-Higgs effective coupling [24], by utilizing an improved non-perturbative function, and by including the effect of the Higgs width.

We also utilize the approximation that the object which couples the gluons to the Higgs (the top quark in the SM) is much heavier than the Higgs itself. This approximation is not essential to our calculation and can be released by including the complete Wilson coefficients with all the relevant masses. The heavy quark approximation in the SM has been shown to be reliable within 5 percent for $m_H < 2m_t$ [25–27], and still reasonable even in the range of $m_H \gtrsim 2m_t$ [21]. It has also been shown that the approximation remains valid for the Q_T distribution in the large Q_T region, provided that $m_H < m_t$ and $Q_T < m_t$ [28]. In this work we assume that the approximation is valid in the whole Q_T region. In the MSSM the heavy quark approximation is also a reliable ansatz for the case of the light Higgs boson and small $\tan\beta$ when the Yukawa coupling of the bottom quark is negligible (c.f. [21] and references therein). Using the CSS formalism we resum large logs of the type $\ln(Q/Q_T)$ in the low Q_T region, and we match the resummed result to the fixed order calculation which is valid for high Q_T [12]. We also include the qg and $q\bar{q}$ subprocesses which, in combination, can constitute up to 10 percent of the total rate, depending on the Higgs mass [25].

The resummed differential cross section of a neutral Higgs boson, denoted by ϕ^0 in the SM or MSSM, produced in hadronic collisions is written as

$$\frac{d\sigma(h_1h_2\to\phi^0X)}{dQ^2\,dQ_T^2\,dy} = \sigma_0\,\frac{Q^2}{S}\,\frac{Q^2\Gamma_\phi/m_\phi}{(Q^2-m_\phi^2)^2+(Q^2\Gamma_\phi/m_\phi)^2}$$
$$\times\left\{\frac{1}{(2\pi)^2}\int d^2b\,e^{i\vec{Q}_T\cdot\vec{b}}\widetilde{W}_{gg}(b_*,Q,x_1,x_2,C_{1,2,3})\right.$$
$$\left.\times\,\widetilde{W}_{gg}^{NP}(b,Q,x_1,x_2)+Y(Q_T,Q,x_1,x_2,C_4)\right\}. \quad (1)$$

The kinematical variables Q, Q_T, and y are the invariant mass, transverse momentum, and rapidity of the Higgs boson, respectively, in the laboratory frame. The parton momentum fractions are defined as $x_1 = e^y M_T/\sqrt{S}$, and $x_2 = e^{-y}M_T/\sqrt{S}$, with $M_T = \sqrt{Q^2+Q_T^2}$, and $\sqrt{S}$ being the center–of–mass (CM) energy of the hadrons h_1 and h_2. The lowest order cross section is

$$\sigma_0 = \kappa_\phi(Q)\frac{\sqrt{2}G_F\alpha_s^2(Q^2)}{576\pi}, \quad (2)$$

where G_F is the Fermi constant, and κ_ϕ, the QCD corrected effective coupling of the Higgs boson to gluons in the heavy top quark limit (cf. Ref. [21]), is defined as

$$\kappa_\phi(Q) = 1+\frac{11}{2}\frac{\alpha_s^{(5)}(m_t^2)}{\pi}+\frac{3866-201\,N_f}{144}\left(\frac{\alpha_s^{(5)}(m_t^2)}{\pi}\right)^2$$
$$+\frac{153-19\,N_f}{33-2\,N_f}\,\frac{\alpha_s^{(5)}(Q^2)-\alpha_s^{(5)}(m_t^2)}{\pi}+\mathcal{O}(\alpha_s^3) \quad (3)$$

where $\alpha_s^{(5)}$ is the strong coupling constant in the $\overline{\rm MS}$ scheme with 5 active flavors, and m_t denotes the pole mass of the top quark.

The renormalization group invariant kernel of the Fourier integral $\widetilde{W}_{gg}(b_*,Q,x_1,x_2,C_{1,2,3})$, and the Q_T regular term $Y(Q_T,Q,x_1,x_2,C_4)$, together with the variables b_* and C_1 to C_4, are given in Ref. [23]. The definition of $\widetilde{W}_{gg}$, contains the Sudakov exponent

$$\mathcal{S}(Q,b_*,C_1,C_2) =$$
$$\int_{C_1^2/b_*^2}^{C_2^2Q^2}\frac{d\overline{\mu}^2}{\overline{\mu}^2}\left[A\left(\alpha_s(\overline{\mu}),C_1\right)\ln\left(\frac{C_2Q^2}{\overline{\mu}^2}\right)+\right.$$
$$\left.B\left(\alpha_s(\overline{\mu}),C_1,C_2\right)\right]. \quad (4)$$

In the perturbative expansion of the $A\left(\alpha_s(\overline{\mu}),C_1\right)$ and $B\left(\alpha_s(\overline{\mu}),C_1,C_2\right)$ functions we follow the notation of Ref. [29]. In our present calculation, we include the process independent next-to-next-to-leading order coefficient

$$A^{(2)}(C_1) = 4C_A\left[\left(\frac{67}{36}-\frac{\pi^2}{12}\right)N_C - \frac{5}{18}N_f - 2\beta_1\ln\left(\frac{b_0}{C_1}\right)\right], \quad (5)$$

in the expansion of the $A\left(\alpha_s(\overline{\mu}), C_1\right)$ function, where $C_A = 3$ is the Casimir of the adjoint representation of $SU(3)$, $N_C = 3$ is the number of colors, and $N_f = 5$ is the number of active quark flavors. With the inclusion of $A^{(2)}$ the only missing next-to-next-to-leading order contribution in the Sudakov exponent is the $B^{(2)}$ term, which is suppressed by $1/\ln\left(\frac{Q^2}{Q_T^2}\right)$ with respect to $A^{(2)}$, and by α_s with respect to $B^{(1)}$. This is illustrated by the expansion of the asymptotic part of the cross section:

$$\lim_{Q_T\to 0}\frac{d\sigma}{dQ^2dQ_T^2dy} = \sigma_0\frac{1}{Q_T^2}\sum_{i,j}\sum_{n=1}^{\infty}\sum_{m=0}^{2n-1}\left(\frac{\alpha_s(Q)}{\pi}\right)^n C_{nm}^{(ij)}\ln^m\left(\frac{Q^2}{Q_T^2}\right), \quad (6)$$

where i and j label incoming partons. While the $A^{(2)}$ coefficient contributes to the above series via

$$C_{21}^{(ij)} \propto -\frac{1}{2}\left[\left(B^{(1)}\right)^2 - A^{(2)} - \beta_0 A^{(1)}\ln\left(\frac{\mu_R^2}{Q^2}\right) - \beta_0 B^{(1)}\right] f_i\, f_j, \quad (7)$$

the $B^{(2)}$ coefficient only occurs as

$$C_{20}^{(ij)} \propto \left[\zeta(3)\left(A^{(1)}\right)^2 + \frac{1}{2}B^{(2)} + \frac{1}{2}\beta_0 B^{(1)}\ln\left(\frac{\mu_R^2}{Q^2}\right)\right] f_i\, f_j, \quad (8)$$

where our notation coincides with that of Ref. [29]. Hence, the contribution from the uncalculated $B^{(2)}$, compared to that from $A^{(2)}$, is expected to be smaller because of the additional log weighting the $A^{(2)}$ coefficient. To estimate the size of the contribution from $B^{(2)}$, we follow the usual practice in a perturbative calculation by varying the renormalization constants (C_1 and C_2) in the Sudakov factor by a factor of 2. The results are shown in Fig. 2.

The form of our non-perturbative function $\widetilde{W}_{gg}^{NP}$ coincides with the one used for the $gg \to \gamma\gamma$ process in Ref. [14]

$$\widetilde{W}_{gg}^{NP}(b, Q, Q_0, x_1, x_2) = \exp\left[-g_1 b^2 - \frac{C_A}{C_F}g_2 b^2\ln\left(\frac{Q}{2Q_0}\right) - g_1 g_3 b\ln\left(100 x_1 x_2\right)\right], \quad (9)$$

where the Casimir of the fundamental $SU(3)$ representation is $C_F = 4/3$. The values of the non-perturbative parameters g_i are defined in Ref. [16]. The uncertainties of the resummed distribution, stemming from the non-perturbative function, were found to be in the order of 5 percent (cf. [30]). In the high Q_T region Eq. (1) is matched to the fixed order perturbative result (at the $\mathcal{O}(\alpha_s)$) of Ref. [27] in the manner described in Ref. [12].

III. NUMERICAL RESULTS

The analytic results are coded in the ResBos Monte Carlo event generator [12,17], which uses the following electroweak input parameters [31]:

$$G_F = 1.16639\times 10^{-5}\ \text{GeV}^{-2}, \quad m_Z = 91.187\ \text{GeV}, \quad m_W = 80.36\ \text{GeV}. \quad (10)$$

As in the background calculation [15], we use the canonical choice of the renormalization constants ($C_1 = C_3 = 2e^{-\gamma_E} \equiv C_0$ and $C_2 = C_4 = 1$ [11]), the NLO expressions for the running electromagnetic and strong couplings $\alpha(\mu)$ and $\alpha_S(\mu)$, as well as the NLO parton distribution function set CTEQ4M (defined in the modified minimal subtraction, $\overline{MS}$, scheme) [32]. We set the renormalization scale equal to the factorization scale: $\mu_R = \mu_F = Q$. In the choice of the non-perturbative parameters, we follow Ref. [16]. Since we are not concerned with the decays of Higgs bosons in this work, we do not impose any kinematic cuts. We defer the more extensive study, including various decay modes and QCD backgrounds, to a future publication Ref. [30].

Fig. 1 displays Higgs boson production cross sections via the gluon fusion process at the LHC, calculated with various QCD corrections in the SM as the function of the Higgs mass. The ratio of the fixed order $\mathcal{O}(\alpha_s^3)$ (dashed) and the lowest order $\mathcal{O}(\alpha_s^2)$ (dotted) curves varies between 2.0 and 2.3. We note that less than 2 percent of the $\mathcal{O}(\alpha_s^3)$ corrections come from the qg and $q\bar{q}$ initial states for Higgs masses below 200 GeV. The resummed curve is about 10 percent higher than the $\mathcal{O}(\alpha_s^3)$ one, as expected based on the findings that the CSS formalism preserves the fixed order rate within the error of the matching (the latter being higher order) [12]. The resummed rate is close to the $\mathcal{O}(\alpha_s^3)$, because we used the $\mathcal{O}(\alpha_s^3)$ fixed order results to derive the Wilson coefficients which are utilized in our calculation. In Ref. [21] a resummed calculation estimated the size of the $\mathcal{O}(\alpha_s^4)$ corrections, and a typical value of 1.5 of the $\mathcal{O}(\alpha_s^4)$ to $\mathcal{O}(\alpha_s^3)$ K-factor can be inferred from that work. Based on this, we also plot the $\mathcal{O}(\alpha_s^3)$ curve rescaled by 1.5, to illustrate the possible size of the $\mathcal{O}(\alpha_s^4)$ corrections and to establish the normalization of our resummed calculation among the fixed order results.

Fig. 2 compares the Higgs boson transverse momentum distributions calculated by ResBos (curves) and by PYTHIA [33] (histograms from version 6.122). The middle solid curve is calculated using the canonical choice

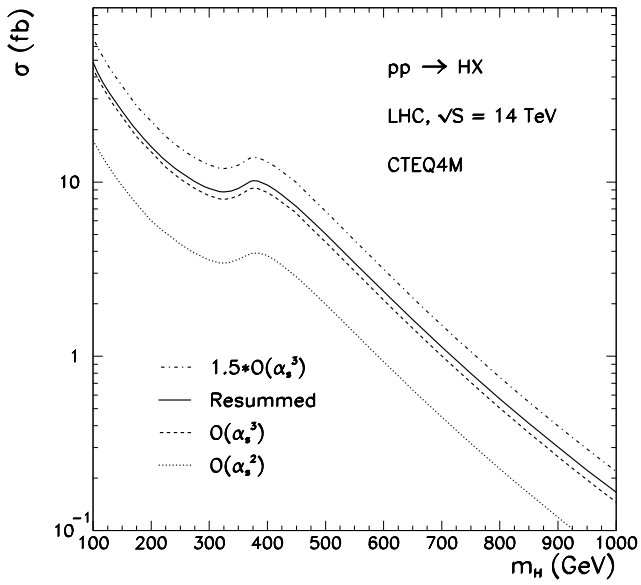

FIG. 1. SM Higgs boson production cross sections at the LHC via gluon fusion as the function of the Higgs mass, with QCD corrections calculated by soft–gluon resummation (solid), at fixed order $\mathcal{O}(\alpha_s^3)$ (dashed), and without QCD corrections at $\mathcal{O}(\alpha_s^2)$ (dotted). The $\mathcal{O}(\alpha_s^3)$ curve is scaled by 1.5 (dash-dotted, c.f. Ref. [21]) to estimate the $\mathcal{O}(\alpha_s^4)$ result.

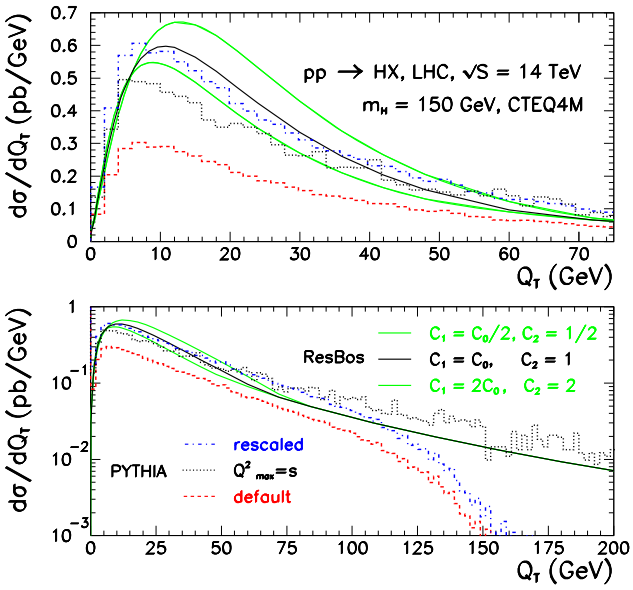

FIG. 2. Higgs boson transverse momentum distributions calculated by ResBos (curves) and PYTHIA (histograms). The default (middle) ResBos curve was calculated with the canonical choice of the renormalization constants, and the other two with doubled (lower curve) and halved (upper curve) values of C_1 and C_2. For PYTHIA we show the original output with default input parameters (dashed), the same rescaled by a factor of $K = 2$ (dotted), and a curve calculated by the altered input parameter value $Q^2_{max} = s$ (dash-dotted). The lower portion, with a logarithmic scale, also shows the high Q_T region.

for the renormalization constants in the Sudakov exponent: $C_1 = C_0$, and $C_2 = 1$. To estimate the size of the uncalculated $B^{(2)}$ term, we varied these renormalization constants multiplying both by $1/2$ and 2. The upper solid curve shows the result for $C_1 = C_0/2, C_2 = 1/2$, and the lower solid curve for $C_1 = 2C_0, C_2 = 2$. The band between these two curves gives the order of the uncertainty following from the exclusion of $B^{(2)}$. The typical size of this uncertainty, e.g. around the peak region, is in the order of ± 10 percent. The corresponding uncertainty in the total cross section is also in the same order. The dashed PYTHIA histogram is plotted without altering its output. The normalization of PYTHIA, as that of any parton shower MCs, is the lowest order $\mathcal{O}(\alpha_s^2)$ for this process. The default PYTHIA histogram is also plotted after the rate is multiplied by the factor $K = 2$ (dotted). The shape of the PYTHIA histogram agrees reasonably with the resummed curve in the low and intermediate Q_T ($\lesssim 125$ GeV) region. For large Q_T the PYTHIA prediction falls under the ResBos curve, since ResBos mostly uses the exact fixed order $\mathcal{O}(\alpha_s^3)$ matrix elements in that region (c.f. Ref. [12]), while PYTHIA still relies on the multi-parton radiation ansatz. PYTHIA can be tuned to agree with ResBos in the high Q_T region (dash-dotted), by changing the maximal virtuality a parton can acquire in the course of the shower, i.e. the Q^2_{max} parameter, from the default value to the partonic center of mass energy s. In that case, however, the low Q_T region will have disagreement, since the normalization in PYTHIA is conserved, so events in the low Q_T region are depleted.

IV. CONCLUSIONS

In this letter we presented Higgs boson production rates and Q_T distributions for the LHC, including $\mathcal{O}(\alpha_s^3)$ fixed order QCD and multiple soft–gluonic corrections by means of the CSS resummation formalism. We showed that the resummed rate recovers the fixed order $\mathcal{O}(\alpha_s^3)$ rate, as expected within the CSS formalism. We investigated the uncertainty of the resummed prediction due to uncalculated terms in the Sudakov exponent. We found that the shape of the resummed prediction in the low Q_T region is in reasonable agreement with the default result of PYTHIA.

ACKNOWLEDGMENTS

We thank the CTEQ Collaboration, and M. Spira for invaluable discussions. We are indebted to I. Puljak for

providing us with the PYTHIA results. C. B. thanks the organizers of the les Houches SUSY/Higgs/QCD workshop for their hospitality and financial support, and the Fermilab Theory Group for their invitation and financial support. This work was supported in part by the NSF under grant PHY–9802564 and by DOE under grant DE-FG-03-94ER40833.

---

[1] M. Felcini, hep-ex/9907049.
[2] Talks given at LEPC, November 9, 1999:
A. Blondel, ALEPH collaboration, http://alephwww.cern.ch/ALPUB/seminar/lepc_nov99/lepc.pdf;
J. Marco, DELPHI collaboration, http://axsant01.cern.ch/lepc;
G. Rahal-Callot, L3 collaboration, http://l3www.cern.ch/conferences/ps/Rahal_LEPC_L3_Nov99.ps.gz;
P. Ward, OPAL collaboration, http://www.cern.ch/Opal/talks/pward_lepc99.ps.gz.
[3] LEP Electroweak Working Group, CERN-EP/99-15 (1999);
P. Langacker, hep-ph/9905428;
G. D'Agostini and G. Degrassi hep-ph/9902226.
[4] B. Abbott *et al.* (D0 Collaboration), Phys. Rev. Lett. **80**, 3008 (1998);
B. Abbott *et al.* (D0 Collaboration), hep-ex/9808029;
F. Abe *et al.* (CDF Collaboration), *Phys. Rev. Lett.* **82**, 271 (1999);
W.M. Yao (CDF Collaboration), hep-ex/9903068;
Y.K. Kim (CDF Collaboration), talk given at *QCD and Weak Boson Physics Workshop*, Fermilab, March 4-6, 1999.
[5] M. Spira, hep-ph/9711394.
[6] ATLAS Collaboration, Technical Proposal, CERN/LHC/94-43 LHCC/P2 (1994);
CMS Collaboration, Technical Proposal, CERN/LHC/94-43 LHCC/P1 (1994);
ATLAS Collaboration, Calorimeter Performance, CERN/LHC/96-40 (1996);
CMS Collaboration, Technical Design Report, CERN/LHCC/97-33 (1997).
[7] S. Abdullin, M. Dubinin, V. Ilyin, D. Kovalenko, V. Savrin, N. Stepanov, *Phys. Lett.* **B431**, 410 (1998).
[8] T. Sjöstrand, Phys. Lett. **157B**, 321 (1985).
[9] A. Kulesza and W.J. Stirling, hep-ph/9909271;
G. Corcella and M.H. Seymour, hep-ph/9908388;
C. Friberg and T. Sjöstrand, hep-ph/9906316;
S. Mrenna, hep-ph/9902471;
G. Miu and T. Sjöstrand, Phys. Lett. **B449**, 313 (1999) hep-ph/9812455.
[10] J.C. Collins and D.E. Soper, Phys. Rev. Lett. **48**, 655 (1982); Nucl. Phys. **B193**, 381 (1981), **B197**, 446 (1982), **B213**, 545(E) (1983).
[11] J.C. Collins, D.E. Soper and G. Sterman, Nucl. Phys. **B250**, 199 (1985).
[12] C. Balázs and C.–P. Yuan, Phys. Rev. **D56**, 5558 (1997) hep-ph/9704258.
[13] F. Landry, R. Brock, G. Ladinsky and C.–P. Yuan, hep-ph/9905391.
[14] C. Balázs, E.L. Berger, S. Mrenna and C.–P. Yuan, Phys. Rev. **D57**, 6934 (1998) hep-ph/9712471.
[15] C. Balázs and C.–P. Yuan, Phys. Rev. **D59**, 114007 (1999) hep-ph/9810319.
[16] C. Balázs, P. Nadolsky, C. Schmidt and C.–P. Yuan, hep-ph/9905551.
[17] C. Balázs, PhD thesis, Michigan State University (1999) hep-ph/9906422.
[18] H. Georgi, S. Glashow, M. Machacek and D.V. Nanopoulos, Phys. Rev. Lett. **40** (1978) 692.
[19] R. P. Kauffman and S. V. Desai, Phys. Rev. **D59**, 057504 (1999), hep-ph/9808286;
R. P. Kauffman, S. V. Desai and D. Risal, Phys. Rev. **D55**, 4005 (1997), hep-ph/9610541.
[20] C. R. Schmidt, Phys. Lett. **B413**, 391 (1997), hep-ph/9707448.
[21] M. Kramer, E. Laenen and M. Spira, Nucl. Phys. **B511**, 523 (1998) hep-ph/9611272.
[22] I. Hinchliffe and S. Novaes, *Phys. Rev.* **D38**, 3475 (1988); R.P. Kauffman, *Phys. Rev.* **D44**, 1415 (1991); *Phys. Rev.* **D45**, 1512 (1992).
[23] C.–P. Yuan, *Phys. Lett.* **B283**, 395 (1992);
[24] B.A. Kniehl and M. Spira, Z. Phys. **C69**, 77 (1995) hep-ph/9505225.
[25] D. Graudenz, M. Spira and P.M. Zerwas, *Phys. Rev. Lett.* **70**, 1372 (1993);
M. Spira, A. Djouadi, D. Graudenz and P.M. Zerwas, *Phys. Lett.* **B318**, 347 (1993);
M. Spira, A. Djouadi, D. Graudenz and P.M. Zerwas, *Nucl. Phys.* **B453**, 17 (1995).
[26] Z. Kunszt, S. Moretti and W.J. Stirling, Z. Phys. **C74**, 479 (1997) hep-ph/9611397.
[27] D. de Florian, M. Grazzini and Z. Kunszt, Phys. Rev. Lett. **82**, 5209 (1999) hep-ph/9902483.
[28] U. Baur and E.W. Glover, Nucl. Phys. **B339**, 38 (1990).
[29] P. B. Arnold and R. P. Kauffman, Nucl. Phys. **B349**, 381 (1991).
[30] C. Balázs and C.–P. Yuan, in preparation.
[31] Particle Data Group (C. Caso *et al.*), *The European Physical Journal* **C 3**, 1 (1998).
[32] H.L. Lai, et al., (CTEQ Collaboration), Phys. Rev. **D55** (1997) 1280.
[33] T. Sjöstrand, Comput. Phys. Commun. **82**, 74 (1994);
L. Lonnblad, Comput. Phys. Commun. **118**, 213 (1999) hep-ph/9810208.